Tightly-Coupled Opportunistic Navigation for Deep Urban and Indoor Positioning

Kenneth M. Pesyna, Jr., Zaher M. Kassas, Jahshan A. Bhatti, and Todd E. Humphreys
The University of Texas at Austin

BIOGRAPHIES

Kenneth M. Pesyna, Jr. is pursuing a Ph.D. in the Department of Electrical and Computer Engineering at The University of Texas at Austin. He received his B.S. in Electrical and Computer Engineering from Purdue University. He is a member of the UT Radionavigation Laboratory and the Wireless Networking and Communications Group. His research interests lie in the area wireless communication and hybrid navigation.

Zaher M. Kassas is pursuing a Ph.D. in the Department of Electrical and Computer Engineering at The University of Texas at Austin. He received his B.E. in Electrical Engineering from The Lebanese American University, M.S. in Electrical and Computer Engineering from The Ohio State University, and M.S.E. in Aerospace Engineering from The University of Texas at Austin. He is a member of the UT Radionavigation Laboratory. His research interests include estimation and filtering, control systems, intelligent autonomous systems (UAVs and UGVs), and navigation.

Jahshan A. Bhatti is pursuing a Ph.D. in the Department of Aerospace Engineering and Engineering Mechanics at the University of Texas at Austin, where he also received his M.S. and B.S. He is a member of the UT Radionavigation Laboratory. His research interests are in the development of small satellites, software-defined radio applications, space weather, and GNSS security and integrity.

Todd E. Humphreys is an assistant professor in the department of Aerospace Engineering and Engineering Mechanics at the University of Texas at Austin and Director of the UT Radionavigation Laboratory. He received a B.S. and M.S. in Electrical and Computer Engineering from Utah State University and a Ph.D. in Aerospace Engineering from Cornell University. His research interests are in estimation and filtering, GNSS technology, GNSS-based study of the ionosphere and neutral atmosphere, and GNSS security and integrity.

ABSTRACT

A strategy is presented for exploiting the frequency stability, transmit location, and timing information of ambient radio-frequency "signals of opportunity" for the purpose of navigating in deep urban and indoor environments. The strategy, referred to as tightly-coupled opportunistic navigation (TCON), involves a receiver continually searching for signals from which to extract navigation and timing information. The receiver begins by characterizing these signals, whether downloading characterizations from a collaborative online database or performing characterizations on-the-fly. Signal observables are subsequently combined within a central estimator to produce an optimal estimate of position and time. A simple demonstration of the TCON strategy focused on timing shows that a TCON-enabled receiver can characterize and use CDMA cellular signals to correct its local clock variations, allowing it to coherently integrate GNSS signals beyond 100 seconds.

I. INTRODUCTION

Tightly-coupled opportunistic navigation (TCON) aims to exploit ambient radio-frequency "signals of opportunity"(SOPs) to assist and enhance conventional global navigation satellite system (GNSS) navigation techniques. "Tightly-coupled" refers to a receiver architecture in which the SOPs are downmixed with the same oscillator and sampled in such a way that a nanosecond-accurate correspondence can be made between the various sampled signal streams. Such coupling enables estimation algorithms to optimally fuse SOP observables at the carrier phase level. "Opportunistic navigation" refers to the strategy of continuously searching for opportune signals from which to extract navigation and timing information, employing on-the-fly signal characterization as necessary. Because it must adapt to the available SOPs, a radionavigation receiver implementing the TCON strategy (a TCON receiver) can be considered a type of cognitive radio [1].

To make discussion and processing of SOPs as general as possible, GNSS and non-GNSS signals are treated equivalently in the TCON framework: all ambient radio signals are considered potential SOPs. Processing of SOPs can be divided notionally into two stages: the characterization stage and the exploitation stage. In the characterization stage, a TCON receiver has recently acquired a new SOP. To optimally combine navigation and timing information extracted from this SOP with information extracted from other SOPs, the signal must first be characterized: trans-

**Preprint of the 2011 ION GNSS Conference
Portland, OR, September 20–23, 2011**

mitter position, timing offset from true time, timing offset rate, and a measure of the carrier stability must all be determined by the receiver. TCON takes a collaborative approach to characterization. A TCON-enabled receiver or "node" wishing to characterize a new SOP can draw *a priori* signal information from an online database of SOP characterizations. The database stores the freshest set of characterizations available for each SOP. Alternatively, SOPs can be characterized on-the-fly by each node individually. Individual nodes may contribute recent SOP characterizations to the database for the benefit of other nodes. In the second SOP processing stage, the TCON receiver exploits the SOP, extracting navigation and timing information provided by the SOP to assist its acquisition and tracking of other SOPs. Once characterized, each SOP acts as a "pseudo-satellite," allowing the TCON receiver to improve its computed position, velocity, and timing (PVT) accuracy by combining all available SOPs. In an environment when GNSS signals are impractically weak or unavailable, navigation may still be possible. Within the TCON framework, receiver position and time can be constrained by tracking the code and carrier phase of whatever SOPs are available.

A TCON receiver's centralized estimator characterizes SOPs and optimally fuses their observables together to produce robust navigation and timing estimates. Several challenges must be addressed in the design of the estimator. First, the estimator must adapt to signals which periodically come and go, implying that the estimator's dynamical model must be of variable state dimension. Second, the estimator must incorporate heterogeneous signals, some of which are more useful for navigation and timing than others. This necessitates an adaptive estimation strategy: the estimator must download SOP models from an online database or characterize these signals and refine its models of them in real-time.

Previous work in the area of hybrid navigation has included fusing together cellular and GPS signals [2], Wi-Fi and GPS signals [3], HDTV and GPS signals [4], and Iridium and GPS signals [5]. Compared to these specific pairings, TCON is a generalization and an optimization: it is designed to *optimally* extract navigation and timing information from *all* available radio-frequency SOPs. By incorporating measurements from a diverse signal set, a TCON receiver can robustly transition between different environments (e.g., outdoor to indoor). By fusing signal measurements at the carrier phase level, a TCON receiver maximizes the navigation and timing-relevant information that it extracts from each signal. Moreover, carrier phase-level signal fusion enables synergistic feedback effects: the TCON receiver's acquisition and tracking sensitivity and robustness for any particular signal is enhanced by observables gathered from other tracked signals. This synergism among signals is the driving rationale behind vector tracking architectures in GNSS receivers [6]. TCON is essentially an extension of vector tracking to include non-GNSS radio signals.

The paper is organized as follows. First, it describes in detail the TCON strategy. Second, it discusses signals of opportunity and desirable characteristics they might have. Third, it presents a centralized estimator to fuse these signal observables together. Finally, a simple TCON demonstration is performed and the results are evaluated followed by conclusions.

II. TCON: A DETAILED DEFINITION

A. Tightly-Coupled

"Tightly-coupled" refers to a receiver architecture in which signals are downmixed and sampled with the same clock and signal observables are fused at the carrier phase level. Referencing all signals to the same clock ensures that identical local clock variations are present in the samples of all targeted signals. This commonality allows the receiver to estimate and remove the effects of its clock variations on its PVT solution. Analog-to-digital conversion of received SOPs must be done in such a way that the TCON receiver can build up a tight correspondence between the sample timing among the various sampled signal streams, even though the sample rates may be different. In some previous hybrid navigation work, GNSS and non-GNSS signals have been downmixed, sampled, and tracked in separate hardware, with timing correspondence provided only by a low-bandwidth inter-hardware link, leading to microsecond-level rms errors in the relative timing of the GNSS and non-GNSS data streams [2]. Such timing uncertainty leads to hundred-meter-level errors when combining pseudorange-type observables in a timing and navigation solution. In contrast, a tightly-coupled architecture enables millimeter-level correspondence in carrier phase measurements among the various tracked SOPs and sub-meter-level correspondence in pseudorange-type measurements. Figure 1 shows a TCON-enabling hardware architecture in which the SOPs—in this case, GNSS, HDTV, and cellular signals—are all signal conditioned and sampled coherently.

To avoid confusion, it should be noted that the notion of tight coupling in the present context does not refer to integration of inertial measurement unit (IMU) measurements and SOP observables [7]. Although it shares many processing similarities with this technique, tight coupling here refers to the fusing of multiple ambient radio signals rather than the fusing of signals with inertial sensors.

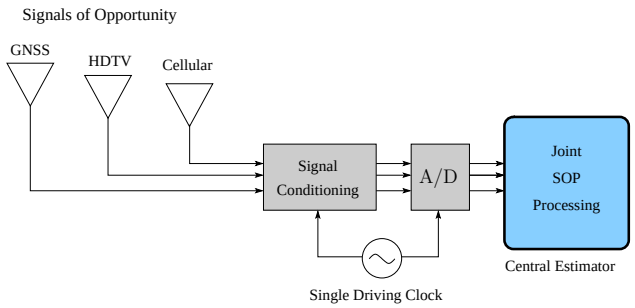

Fig. 1. One implementation of a TCON-enabled receiver.

B. Opportunistic Navigation

"Opportunistic navigation" refers to a strategy in which a TCON receiver is continuously searching for ambient signals from which to extract navigation and timing information. A receiver may choose to search out all available signals or concentrate on a specific subset. Section III will present and describe various potential SOPs. To make use of the available SOPs, a TCON receiver must characterize the SOP by determining its carrier stability, timing offset from true time, timing offset rate, transmitter location, and carrier-to-noise (C/N_0) ratio. A TCON receiver can perform SOP characterization on-the-fly as a standalone process. Alternatively, for improved performance, the TCON receiver may draw from an up-to-date SOP characterization database to which it and other TCON receivers contribute collaboratively. The database is "smart" in that it delivers upon request an SOP characterization complete with SOP parameters and associated probability distributions that have been brought up-to-date by the database's internal SOP dynamics model. This networked version of TCON is an example of decentralized collaborative PVT estimation.

III. SIGNALS OF OPPORTUNITY

TCON treats all radio-frequency signals as potential signals of opportunity. This includes GNSS signals such as GPS, Galileo, and Glonass; cellular signals such as CDMA, GSM, 4G LTE, and WiMAX; high-definition television (HDTV), Wi-Fi, and non-GNSS satellite signals such as broadcast by the Iridium communication system.

A. Desirable SOP Characteristics

SOPs are most useful in the TCON framework if they have the following desirable characteristics:

Known (or predictable) timing offset from true time: Standard time-of-arrival (TOA)-based navigation depends on one knowing—or being able to predict via some deterministic model—the transmission time of features in received signals. For example, in the case of GPS signals, the true transmission time of the start of a spreading code sequence can be calculated based on timing parameters broadcast in the navigation data. Because a transmitter-applied time stamp can usually be inferred from the received SOPs, knowing the transmit time of a particular signal feature is equivalent to knowing the transmitter clock's offset from true time.

Stable transmitter clock: The more stable the SOP transmitter clock, the less often a corresponding clock error model needs to be updated in a TCON receiver. For example, to support long coherent integration of an SOP signal driven by a low-cost temperature-compensated crystal oscillator (TCXO), an update of the TCXO's error model parameters would be required every 100 milliseconds or so. In contrast, the parameters of GPS satellite clock error models need only be updated every 2 hours.

Known (or predictable) location: TOA-based navigation also depends on one knowing—or being able to predict—the transmitter location at any given time.

High received signal power: The received signal power depends on the effective isotropic radiated power (EIRP), the signal wavelength, the receiver-transmitter distance, any intervening signal-attenuating material, and the receiver hardware. Naturally, higher received power yields more precise observables.

Wide bandwidth: Wider bandwidth signals offer better precision in TOA measurements and better immunity to multipath effects.

Continuous carrier: A continuous carrier underlying an SOP permits long coherent integration and facilitates carrier-based positioning.

Known signal structure: Generation of a local signal replica for tracking purposes requires knowledge of the SOP signal structure. While it is true that the signal carrier can be recovered without knowledge of the signal structure (e.g., by squaring techniques), the penalty paid for such techniques is increased squaring loss.

B. "Freestyle" Navigation

In practice, available SOPs will lack some of these desirable characteristics. This is especially true of communication signals, most of which were not designed with navigation in mind. As an illustration of this, consider the navigation-and-timing-relevant characteristics of the following example SOPs:

1. GPS Signals

(a) Low received signal power ($\sim$ –150 dBW)
(b) High frequency stability ($\sim 10^{-12}$)
(c) Known transmitter location via broadcast ephemeris
(d) Known transmitter timing offset via broadcast clock model

2. Code Division Multiple Access (CDMA) Cellular
(a) High received signal power relative to GPS ($\sim$ –110 dBW)
(b) Varying frequency stability from provider to provider ($\sim 10^{-10}$ to 10^{-11})
(c) Static tower location, although not always known
(d) Rough synchronization to GPS time (μs-level errors)

3. Iridium Satellite System
(a) High received signal power relative to GPS ($\sim$ –130 dBW)
(b) Good frequency stability ($\sim 10^{-10}$ to 10^{-11})
(c) Freely available ephemeris (via NORAD TLEs) with rough accuracy ($\sim$ 100m)
(d) Unknown clock offset relative to true time
(e) Non-continuous carrier due to TDMA structure
(f) Ambiguous carrier phase from burst to burst

Despite the few unfavorable characteristics of the CDMA cellular and Iridium signals, a TCON receiver can make effective use of them. The same holds true for many other SOPs. The key to dealing with less-than-ideal SOPs is an ability to adapt, to characterize signals on-the-fly as they become available or to draw an applicable characterization from an SOP characterization database, as described earlier. In this paradigm, which might be called "freestyle navigation," a TCON receiver refines its estimate of SOP characterization parameters even while refining an estimate of its own PVT. The centralized estimator described in the following section makes this simultaneous estimation possible.

IV. CENTRALIZED ESTIMATOR

The purpose of the centralized estimator is to optimally combine observables from all SOPs targeted by a TCON receiver. In this work, the centralized estimator is implemented as an extended Kalman filter (EKF). The following subsections describe the filter's state vector, measurement models, and dynamics models.

A. State Vector

The estimator's state vector concatenates a receiver base state $\mathbf{x}_{\text{receiver}}$ with a state $\mathbf{x}_{\text{SOP}}$ for each SOP. The base state

$$\mathbf{x}_{\text{receiver}} = \begin{bmatrix}\mathbf{r}^{\mathsf{T}} & \delta t & \dot{\mathbf{r}}^{\mathsf{T}} & \dot{\delta t}\end{bmatrix}^{\mathsf{T}} \tag{1}$$

consists of the receiver's three-dimensional position $\mathbf{r}$, the receiver's three-dimensional velocity $\dot{\mathbf{r}}$, the time offset of the receiver's clock δt, and the time derivative of this offset, also known as receiver's clock drift $\dot{\delta t}$. The SOP state

$$\mathbf{x}_{\text{SOP}} = \begin{bmatrix}\mathbf{r}_{\text{SOP}}^{\mathsf{T}} & \delta t_{\text{SOP}} & \dot{\delta t}_{\text{SOP}} & \gamma_{\text{SOP}}\end{bmatrix}^{\mathsf{T}} \tag{2}$$

consists of the SOP's three-dimensional position $\mathbf{r}_{\text{SOP}}$, the SOP's clock offset from true time δt_{SOP}, the SOP's clock drift $\dot{\delta t}_{\text{SOP}}$, and the SOP carrier phase ambiguity term γ_{SOP}. As the TCON receiver discovers SOPs, the base state vector is augmented with SOP states to match the number of SOPs being tracked. This augmented base state forms the full state vector

$$\mathbf{x} = \begin{bmatrix}\mathbf{x}_{\text{receiver}}^{\mathsf{T}}, & \mathbf{x}_{\text{SOP}_1}^{\mathsf{T}}, & \mathbf{x}_{\text{SOP}_2}^{\mathsf{T}}, \ldots, \mathbf{x}_{\text{SOP}_N}^{\mathsf{T}}\end{bmatrix}^{\mathsf{T}} \tag{3}$$

For some SOPs with well-known parameters, only a subset of the usual elements will be included in $\mathbf{x}_{\text{SOP}}$. For example, if the SOP transmitter position is known, as is the case with GPS satellites or, on occasion, with cellular basestations, then the position $\mathbf{r}_{\text{SOP}}$ can be omitted from the SOP's state vector. Likewise, if the transmitter clock error parameters are provided to the receiver, as is the case with GPS signals, then δt_{SOP} and $\dot{\delta t}_{\text{SOP}}$ can be omitted. In these cases of known SOP parameters, the full $\mathbf{x}_{\text{SOP}}$ state could be retained and the Kalman filter initialized with precise *a priori* estimates of the known quantities, but this approach is more computationally demanding than omitting the SOP parameters that can be accurately predicted by a deterministic model, whether the model is drawn from broadcast data or from an online database.

B. Carrier Phase Measurement Models

The TCON central estimator is designed to ingest both carrier phase and pseudorange-type SOP measurements. Models for these measurements are similar to standard GPS carrier phase and pseudorange models, with some important distinctions. To illustrate these distinctions the following subsections present GPS, CDMA, and Iridium carrier phase measurement models.

B.1 GPS Carrier Phase Measurement Model

The GPS beat carrier phase $\phi_G(t_R)$, in cycles, at receiver time t_R can be modeled as [8]

$$\begin{aligned}\phi_G(t_R) = \frac{1}{\lambda}||\underline{\underline{\mathbf{r}(t_R)}} - \mathbf{r}_{SV}(t_R - \delta t(t_R) - \delta t_{TOF})|| \\ + \frac{c}{\lambda}[\underline{\underline{\delta t(t_R)}} - \delta t_{SV}(t_R - \delta t(t_R))] + \underline{\underline{\gamma_G}} \\ + \epsilon_{iono}(t_R) + \epsilon_{tropo}(t_R) + \nu_{\phi_G}(t_R)\end{aligned} \tag{4}$$

The terms that are underlined are initially unknown and thus are included in the SOP state vector. For GPS signals, this includes the receiver position $\mathbf{r}(t_R)$, the receiver clock

offset $\delta t(t_R)$, and the carrier phase constant γ_G. Other terms such as the satellite position $\mathbf{r}_{SV}$ and the satellite clock offset δt_{SV} can be accurately predicted based on the broadcast navigation data. A substantial component of the ionospheric and tropospheric phase errors $\epsilon_{iono}(t_R)$ and $\epsilon_{tropo}(t_R)$ can also be eliminated by the broadcast model, by dual-frequency measurements, or by ionospheric and tropospheric models available on the Internet. $\nu_{\phi_G}(t_R)$ represents additive white thermal noise introduced by the receiver front end. Constants representing the speed-of-light c and the GPS-signal wavelength λ are present to convert all terms to units of cycles, and the GPS-signal time-of-flight δt_{TOF} is present to refer the satellite position $\mathbf{r}_{SV}$ to the time of signal transmission.

B.2 CDMA Carrier Phase Measurement Model

The beat carrier phase measurement model of CDMA cellular signals is similar to that of the GPS carrier phase model. The CDMA beat carrier phase $\phi_C(t_R)$, in cycles, at receiver time t_R can be modeled as

$$\begin{aligned}\phi_C(t_R) =& \frac{1}{\lambda}||\underline{\underline{\mathbf{r}(t_R)}} - \underline{\underline{\mathbf{r}_C}}|| + \frac{c}{\lambda}[\underline{\underline{\delta t(t_R)}} \\ & - \underline{\underline{\delta t_C(t_R - \delta t(t_R))}}] + \underline{\underline{\gamma_C}} + \nu_{\phi_C}(t_R)\end{aligned} \tag{5}$$

The CDMA carrier phase model is different from the GPS carrier phase model in three respects: First, the constant CDMA transmitter (basestation) position $\mathbf{r}_C$ may not be known to the receiver. In this case $\mathbf{r}_C$ must be included in the corresponding $\mathbf{x}_{\text{SOP}}$ and estimated on-the-fly. Typically, however, an accurate estimate of $\mathbf{r}_C$ could be drawn from the SOP characterization database and thus $\mathbf{r}_C$ could be omitted from $\mathbf{x}_{\text{SOP}}$. Second, the transmitter's clock offset δt_C may not be known to the receiver. Although a model for δt_C may be drawn from the SOP characterization database, the model may not be sufficiently accurate to omit δt_C from $\mathbf{x}_{\text{SOP}}$. Third, the CDMA carrier phase model does not include ionospheric or tropospheric error terms, as these are negligible for ground-based cellular transmissions.

B.3 Iridium Carrier Phase Measurement Model

The Iridium satellite system is a constellation of 66 low Earth orbit (LEO) satellites which provide global communication coverage. There has been significant research in the use of Iridium as a complement to GPS in jamming and otherwise GPS-denied environments, such as deep indoors [5]. The beat carrier phase $\phi_I(t_R)$, in cycles, of an Iridium signal at receiver time t_R can be modeled as

$$\phi_I(t_R) = \begin{cases} \frac{1}{\lambda}||\underline{\underline{\mathbf{r}(t_R)}} - \mathbf{r}_I(t_R - \delta t(t_R) - \delta t_{TOF})|| \\ +\frac{c}{\lambda}[\underline{\underline{\delta t(t_R)}} - \underline{\underline{\delta t_I(t_R - \delta t(t_R))}}] + \underline{\underline{\gamma_I}} \\ +\frac{1}{M}\underline{\underline{\eta(t_R - \delta t(t_R) - \delta t_{TOF})}} + \epsilon_{iono}(t_R) \\ +\epsilon_{tropo}(t_R) + \nu_{\phi_I}(t_R), & \text{within a burst} \\ 0, & \text{between bursts} \end{cases} \tag{6}$$

The Iridium carrier phase model has two key differences from that of the GPS carrier phase model. The first is the piecewise nature of $\phi_I(t_R)$. The Iridium signal is transmitted as a time division multiple access (TDMA) waveform. These waveforms are burst-like, with the signal on during a burst and off between bursts. Within a burst, the carrier phase is observable as shown in Eq. (6); between bursts, no power is transmitted. The second key difference is the $\frac{1}{M}\eta$ term, which is present to model the random fractional-cycle phase ambiguity introduced by the satellite at the beginning of each burst.

To make use of the Iridium signal within the TCON framework, a continuous carrier phase time history can be stitched together from the glimpses of this time history provided within each burst. As part of this processing, the random fractional-cycle ambiguities can be resolved. This phase-stitching and ambiguity resolution process can be done within the Kalman filter if η, the integer part of the ambiguity, is added to the SOP state, and the filter is modified to estimate both real-valued states and this integer-valued ambiguity. This phase-stitching and ambiguity resolution algorithm has been the subject ongoing research by the authors and will be the topic of a future paper.

C. Dynamics Model

The state dynamics for the TCON extended Kalman filter can be modeled as

$$\mathbf{x}(k{+}1) = \mathbf{\Phi}(k)\mathbf{x}(k){+}\mathbf{\Gamma}(k)\mathbf{w}(k), \;\; \mathbf{w}(k) \sim \mathcal{N}(\mathbf{0}, \mathbf{Q}(k)) \tag{7}$$

where $\mathbf{x}$ is the system state, $\mathbf{w}$ is the process noise, $\mathbf{\Phi}$ is the state transition matrix, $\mathbf{\Gamma}$ is the process noise coefficient matrix, and $\mathbf{Q}$ is the process noise covariance matrix. The state dynamics are governed by a simple polynomial model, as shown below for an example case in which a single SOP is present:

The estimator has the full state vector

$$\begin{aligned}\mathbf{x} &= \left[\mathbf{x}_{\text{receiver}}^{\mathsf{T}}, \mathbf{x}_{\text{SOP}}^{\mathsf{T}}\right]^{\mathsf{T}} \\ &= \left[\mathbf{r}^{\mathsf{T}}, \delta t, \dot{\mathbf{r}}^{\mathsf{T}}, \dot{\delta t}, \mathbf{r}_{\text{SOP}}^{\mathsf{T}}, \delta t_{\text{SOP}}, \dot{\delta t}_{\text{SOP}}, \gamma_{\text{SOP}}\right]^{\mathsf{T}}\end{aligned} \tag{8}$$

the state transition matrix

$$\mathbf{\Phi}(k) = \begin{bmatrix} \mathbf{I}_{3\times3} & \mathbf{0} & \mathrm{T}\cdot\mathbf{I}_{3\times3} & \mathbf{0} & \mathbf{0} & \mathbf{0} & \mathbf{0} & \mathbf{0} \\ \mathbf{0} & 1 & \mathbf{0} & \mathrm{T} & \mathbf{0} & 0 & 0 & 0 \\ \mathbf{0} & \mathbf{0} & \mathbf{I}_{3\times3} & \mathbf{0} & \mathbf{0} & \mathbf{0} & \mathbf{0} & \mathbf{0} \\ \mathbf{0} & 0 & \mathbf{0} & 1 & \mathbf{0} & 0 & 0 & 0 \\ \mathbf{0} & \mathbf{0} & \mathbf{0} & \mathbf{0} & \mathbf{I}_{3\times3} & \mathbf{0} & \mathbf{0} & \mathbf{0} \\ \mathbf{0} & 0 & \mathbf{0} & 0 & \mathbf{0} & 1 & \mathrm{T} & 0 \\ \mathbf{0} & 0 & \mathbf{0} & 0 & \mathbf{0} & 0 & 1 & 0 \\ \mathbf{0} & 0 & \mathbf{0} & 0 & \mathbf{0} & 0 & 0 & 1 \end{bmatrix} \quad (9)$$

where T represents the amount of time between consecutive filter updates; the process noise coefficient matrix

$$\mathbf{\Gamma}(k) = \mathbf{I}_{14\times14}, \quad (10)$$

and the process noise covariance matrix

$$\boldsymbol{Q} = \begin{bmatrix} [{\sigma_{\mathbf{r}}}^2] & \mathbf{0} & \mathbf{0} & \mathbf{0} & \mathbf{0} & \mathbf{0} & \mathbf{0} & \mathbf{0} \\ \mathbf{0} & \sigma^2_{\delta t} & \mathbf{0} & \sigma^2_{\delta t\dot{\delta} t} & \mathbf{0} & 0 & 0 & 0 \\ \mathbf{0} & \mathbf{0} & [{\sigma_{\dot{\mathbf{r}}}}^2] & \mathbf{0} & \mathbf{0} & \mathbf{0} & \mathbf{0} & \mathbf{0} \\ \mathbf{0} & \sigma^2_{\delta t\dot{\delta} t} & \mathbf{0} & \sigma^2_{\dot{\delta} t} & \mathbf{0} & 0 & 0 & 0 \\ \mathbf{0} & \mathbf{0} & \mathbf{0} & \mathbf{0} & [{\sigma_{\mathbf{r_S}}}^2] & \mathbf{0} & \mathbf{0} & \mathbf{0} \\ \mathbf{0} & 0 & \mathbf{0} & 0 & \mathbf{0} & \sigma^2_{\delta t_S} & \sigma^2_{\delta t_S\dot{\delta} t_S} & 0 \\ \mathbf{0} & 0 & \mathbf{0} & 0 & \mathbf{0} & \sigma^2_{\delta t_S\dot{\delta} t_S} & \sigma^2_{\dot{\delta} t_S} & 0 \\ \mathbf{0} & 0 & \mathbf{0} & 0 & \mathbf{0} & 0 & 0 & \sigma^2_{\gamma_S} \end{bmatrix} \quad (11)$$

The process noise $\mathbf{w}(k)$ accounts for any unmodeled dynamics in the state and is assumed to be Gaussian distributed with mean 0 and covariance $\mathbf{Q}$. $\mathbf{Q}$ defines the noise covariances for each component of the state. $[\sigma^2_{\mathbf{r}}]$ and $[\sigma^2_{\mathbf{r}_{\mathrm{SOP}}}]$ refer to the noise covariance matrices for the position of the receiver $\mathbf{r}$ and the position of the SOP $\mathbf{r_S}$. The covariance values within these matrices are sized to account for any unmodeled position changes. Most SOPs are assumed static (e.g. cellular basestations) or are assumed to have known trajectories (e.g. GPS satellites). Additionally, any changes in the receiver's position is assumed to be well modeled by its velocity. As a result, these position process noise covariances can be kept much less than 1 m^2. The noise covariance matrix of the receiver's velocity $[\sigma^2_{\dot{\mathbf{r}}}]$ accounts for any unmodeled changes in the velocity of the receiver between consecutive filter updates. Since acceleration is not part of the state, the covariances within this matrix should be sized to account for the expected level of randomness in velocity.

The remaining terms, $\sigma^2_{\delta t}$, $\sigma^2_{\dot{\delta} t}$, $\sigma^2_{\delta t\dot{\delta} t}$, $\sigma^2_{\delta t_S}$, $\sigma^2_{\dot{\delta} t_S}$, and $\sigma^2_{\delta t_S\dot{\delta} t_S}$ account for receiver and SOP clock noise. Often a receiver has a good estimate of the variations of its own clock, and thus the receiver clock terms $\sigma^2_{\delta t}$, $\sigma^2_{\dot{\delta} t}$, and $\sigma^2_{\delta t\dot{\delta} t}$ are well-known in advance. However, the SOP clock terms $\sigma^2_{\delta t_S}$, $\sigma^2_{\dot{\delta} t_S}$, and $\sigma^2_{\delta t_S\dot{\delta} t_S}$ will either need to be downloaded from a database as new SOPs are acquired or determined on-the-fly. This on-the-fly calibration, if performed, motivates the need for an adaptive dynamics model where the process noise covariance associated with the SOP clocks is refined iteratively as explained in the next section.

D. Adaptive Dynamics Model: Process Noise Covariance

To process SOP observables correctly, the Kalman filter needs a good estimate of the SOP clock dynamics to include as part of its process noise covariance matrix $\mathbf{Q}$. But if the receiver has no knowledge about the SOP, how is it to provide the filter with a good *a priori* model of its clock dynamics? The receiver could draw from an online SOP characterization database as discussed in sec. II-B or it could perform a standalone characterization on-the-fly. For on-the-fly characterization, the receiver must provide an initial guess of the model to the filter and then iteratively converge on a more accurate estimate through the approach presented in Fig. 2.

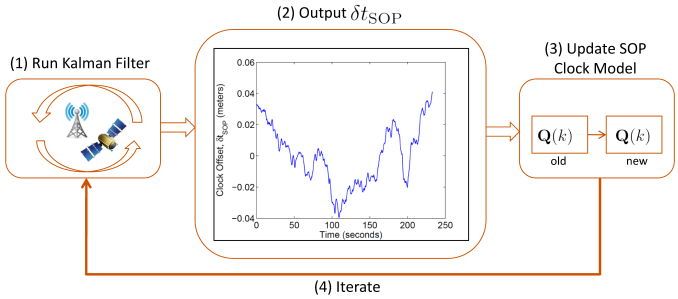

Fig. 2. The filter characterizes the SOP by iteratively estimating the SOP clock dynamics and updating the process noise covariance matrix $\mathbf{Q}$ with new clock model parameters.

In this approach, the Kalman filter starts with an initial guess of $\mathbf{Q}$. Using this guess, the filter begins to process observables, outputting an estimate phase-time history of the SOP clock offset $\hat{\delta}_{\mathrm{SOP}}(t)$ as part of its state estimate. Under conditions of strong observability (e.g., ≥ 4 GPS satellites tracked and a known transmitter location for the target SOP), $\hat{\delta}_{\mathrm{SOP}}(t)$ will be close to the true SOP clock offset $\delta_{\mathrm{SOP}}(t)$ despite the presence of modest modeling errors in $\mathbf{Q}$. The accuracy of $\hat{\delta}_{\mathrm{SOP}}(t)$ under these conditions implies that improved clock model parameters for the target SOP can be obtained by an analysis of $\hat{\delta}_{\mathrm{SOP}}(t)$. These parameters are fed into a refined $\mathbf{Q}$ and the process is repeated until convergence.

Although this iterative approach has been shown to work under conditions of strong observability, it is not statistically rigorous and does not degrade gracefully under conditions of weak observability. Future implementations of the TCON central estimator will adopt the adaptive approach of Ref. [9], in which $\mathbf{Q}$ is refined by combining weighted

candidate models that are tested simultaneously in a multiple model framework.

E. Importance of Backward Smoothing

Within the TCON framework, there is a need to implement backward-smoothing in addition to regular forward filtering. New measurements create innovations within a (causal) filter which introduce abrupt dynamics in the filtered state estimates. These abrupt dynamics may not conform to the filter's state dynamics model, even when the filter's assumed dynamics and measurement models are an accurate reflection of reality [10]. Backward smoothing removes the abrupt dynamics introduced by innovations in forward-pass filtering. In other words, smoothing more accurately recreates the actual signal dynamics, allowing the state variations to conform more closely to the *a priori* dynamics model. There are certain state elements for which smoothing is critically necessary. The receiver clock offset δt is one such element. An accurate estimate of δt is needed to perform long coherent integrations in weak-signal environments for purposes of signal detection. A smoothed $\delta t(t_R)$ time history eliminates the need for ad-hoc frequency stability transfer techniques such as the one advanced in [11].

Figure 3 shows the effects of smoothing versus filtering on the time history of the receiver clock estimate $\delta t(t_R)$ for a single run of the Kalman filter and backward-smoother while ingesting carrier phase observables from six GPS satellites. It is apparent from this figure that the filtered estimate of $\delta t(t_R)$ varies much more wildly than the smoothed estimate. Consequently, the filtered estimate does not conform to expected clock variations modeled in $\mathbf{Q}$ whereas the smoothed estimate does.

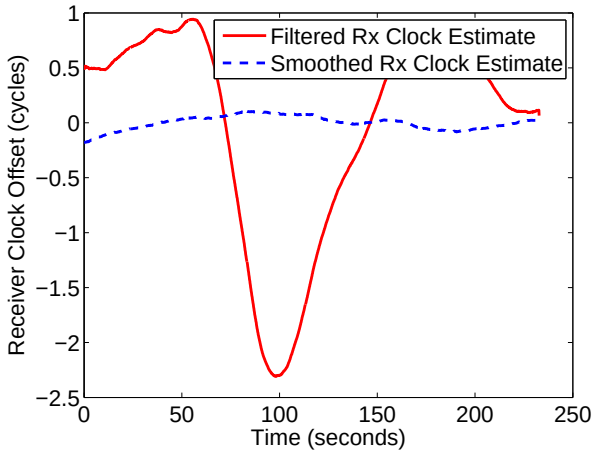

Fig. 3. Filtered and smoothed estimates of δt produced by the Kalman filter while ingesting carrier phase observables from six GPS satellites.

V. SIMPLE TCON DEMONSTRATION

This section describes a simple demonstration designed to show the benefits of TCON. Although one of the main uses of TCON is for navigation, this demonstration will focus on timing. The goal of this demonstration is to show how a TCON receiver calculates its receiver clock variations using two types of SOPs: GPS signals and cellular CDMA signals.

A. Experimental Setup

The experimental setup is presented in Fig. 4. Two National Instruments RF Vector Signal Analyzers (RFSAs) were used to simultaneously downmix and sample both GPS and CDMA signals. Both RFSAs were driven by the same external reference clock and sampled synchronously, in compliance with the tightly-coupled requirement of the TCON framework. The samples were stored to a redundant array of independent disks (RAID). Next, the Generalized Radionavigation Interfusion Device (GRID) software receiver [12, 13] was augmented to simultaneously track both the GPS L1 C/A and CDMA cellular pilot signals. The receiver was programmed to produce simultaneous pseudorange and carrier phase observables at a rate of 10 Hz for 6 of the GPS satellites in view as well as two CDMA basestations. Finally, these observables were fed into a centralized estimator, a MATLAB-based extended Kalman filter, where they were optimally fused to estimate the elements of the full state presented in Eq. (12).

$$\mathbf{x} = \left[\mathbf{x}_{\text{rec.}}^{\mathsf{T}}, \mathbf{x}_{\text{GPS}_1}^{\mathsf{T}}, \ldots, \mathbf{x}_{\text{GPS}_6}^{\mathsf{T}}, \mathbf{x}_{\text{CDMA}_1}^{\mathsf{T}}, \mathbf{x}_{\text{CDMA}_2}^{\mathsf{T}}\right]^{\mathsf{T}} \quad (12)$$

The SOP state vector for each tracked GPS signal $\mathbf{x}_{\text{GPS}}$ is a subset of the full SOP state vector $\mathbf{x}_{\text{SOP}}$. As discussed in section IV-A, $\mathbf{r}_{\text{SOP}}$, δt_{SOP}, and $\dot{\delta t}_{\text{SOP}}$ can be omitted from $\mathbf{x}_{\text{SOP}}$ for GPS signals since they can be accurately predicted from models drawn from the GPS broadcast data. The only unknown state element for GPS signals that needs to be estimated by the filter and is thus contained in $\mathbf{x}_{\text{GPS}}$ is the GPS carrier phase ambiguity term γ_{GPS}. The SOP state vector for each tracked CDMA signal $\mathbf{x}_{\text{CDMA}}$ consists of a subset of $\mathbf{x}_{\text{SOP}}$ as well. In this demonstration, is is not necessary to know or estimate the positions of the CDMA transmitters. Thus $\mathbf{r}_{\text{CDMA}}$ is omitted from $\mathbf{x}_{\text{CDMA}}$. The other three CDMA SOP state parameters δt_{CDMA}, $\dot{\delta t}_{\text{CDMA}}$, and γ_{CDMA} must be estimated and thus are included in $\mathbf{x}_{\text{CDMA}}$.

B. Wardriving for Signals of Opportunity

Signals for this demonstration were captured during a wardriving effort in downtown Austin, Texas. The National Instruments equipment and the RAID (Fig. 4.(1)) were placed into a vehicle (Fig. 5), and two antennas

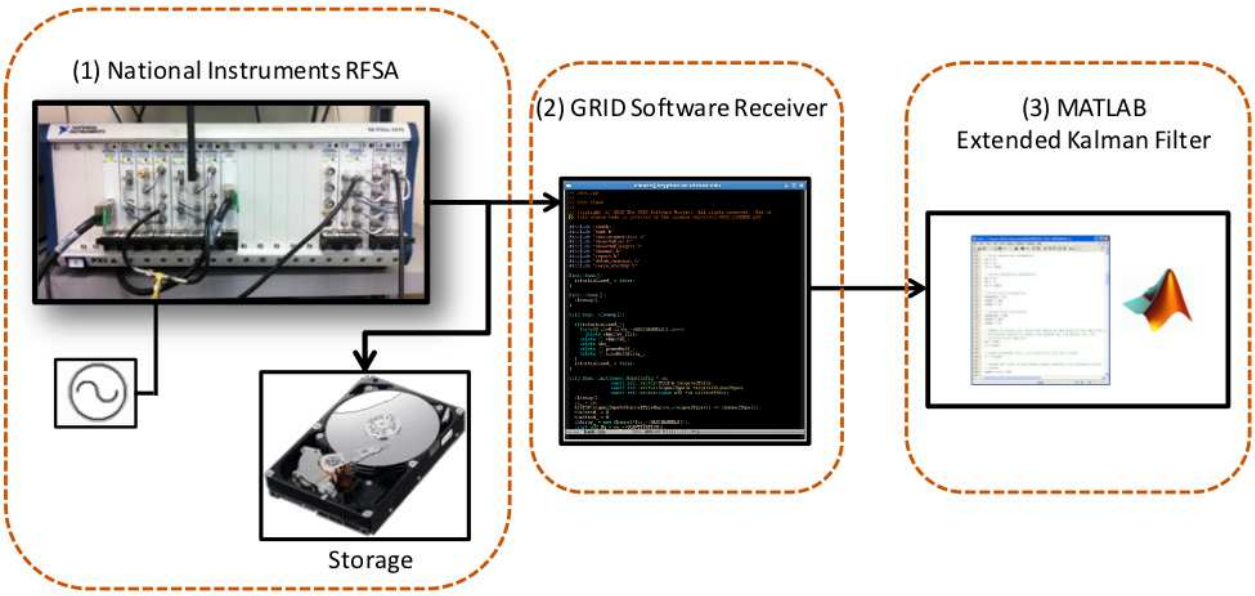

Fig. 4. The TCON experimental setup: (1) Sample CDMA and GPS signals using two National Instruments RFSAs and store the sampled data to a RAID. (2) Track both signals and produce observables using the GRID software receiver. (3) Fuse these observables together within a MATLAB-based EKF.

were placed on the roof of the vehicle (Fig. 6). One antenna was designed to capture GPS signals and the other CDMA signals. Signals were recorded in static, dynamic,

Fig. 5. The National Instruments RFSAs, RAID, reference clock, and computer placed in the back of the wardriving vehicle.

"open sky," and "dense urban" situations. For this timing demonstration, the data from one of the "static, open sky" situations were used. Specifically, the vehicle was parked along the side of the road (Fig. 7) and signals from two cell basestations, a Sprint and a Verizon basestation, were recorded simultaneously along with signals from all GPS satellites in view.

Fig. 6. Wardriving antennas placed on the roof of the vehicle.

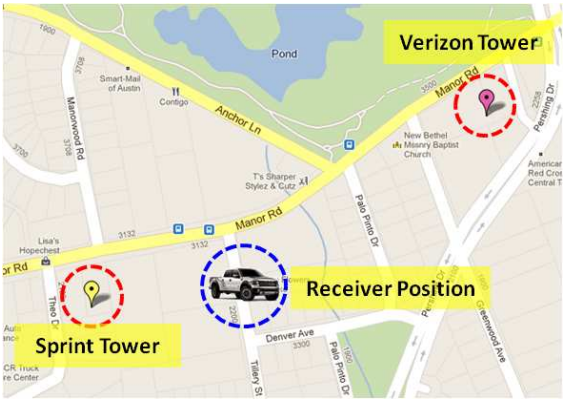

Fig. 7. Vehicle and tower positions for the "static, open-sky" signal recording.

C. Results: Estimating Receiver Clock Dynamics

The data from the wardriving effort were post-processed within the GRID software receiver (Fig. 4.(2)) to produce carrier phase observables for six GPS satellites and two

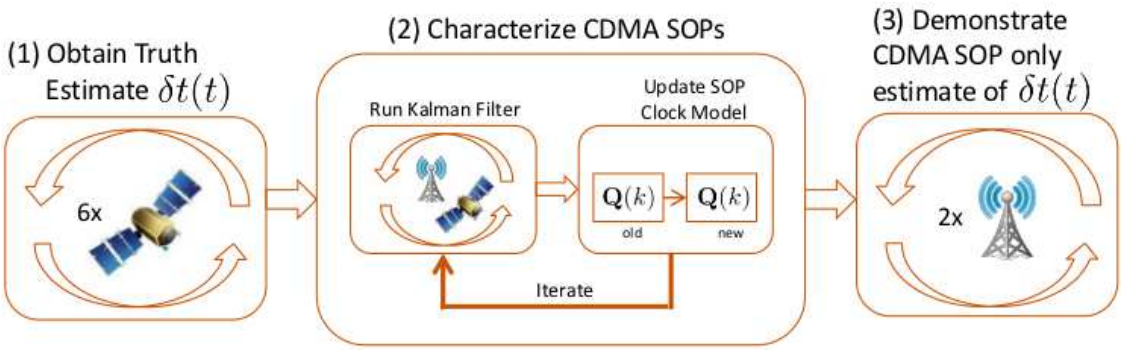

Fig. 8. Three processing stages of the TCON demonstration: (1) Obtain a "truth" estimate of the local clock variations $\delta t(t)$ by ingesting only GPS observables into the EKF. (2) Characterize CDMA SOPs by ingesting both CDMA and GPS observables. (3) Estimate $\delta t(t)$ ingesting only CDMA observables.

CDMA basestations. These observables were subsequently fed into an extended Kalman filter (EKF) implemented in MATLAB (Fig. 4.(3)).

The EKF was run in three stages. In the first stage, it ingested GPS carrier phase observables from the six GPS satellites. In the second stage, it ingested both the GPS observables as well as carrier phase observables from the two cellular CDMA basestations. In the third stage, it ingested only CDMA carrier phase observables. These three stages are diagrammed in Fig. 8. In all three stages the forward-pass filter was run followed by the backward-smoother. As explained in section IV-E, the backward-smoother produces state estimates which conform more closely to the dynamics model.

During the first stage, the smoother estimated the carrier phase ambiguity term γ_{GPS} for each GPS satellite. As described in section V-A, this is the only SOP state parameter that needs to be estimated for GPS signals. During this stage, the smoother also estimated the receiver's position $\mathbf{r}$ as well as the receiver's clock offset and drift, δt and $\dot{\delta t}$. Given the strong observability afforded by tracking six GPS signals, the smoother's estimates of the receiver's position and clock dynamics were very accurate. For the sake of this demonstration and the results to come, the smoother's estimate of the receiver clock offset as a function of receiver time $\hat{\delta t}(t_R)$ is taken as the "truth" time history of δt.

During the second stage, while ingesting both GPS and CDMA measurements, the smoother was set to perform an on-the-fly characterization of signals from the two CDMA basestations. The smoother iterated over the same segment of data until it converged on a process noise model for each CDMA SOP clock. It also calculated the carrier phase ambiguity term γ_{CDMA} for each basestation.

During the final stage, the smoother was evaluated for its ability to estimate the receiver clock offset while ingesting only CDMA observables. This shall be called the CDMA-only based estimate $\hat{\delta t}_{\text{CDMA}}$ of δt. Here, the smoother exploited the characterization of the CDMA SOPs performed during stage 2. Because of this characterization the smoother knew precisely how to weight the carrier phase measurements from each SOP. This is significant because it was found that the Verizon SOP was significantly more stable than the Sprint SOP.

Figures 9 and 10 show a comparison, at each stage, of the smoother's estimate of the receiver clock variations for two different receiver clocks. Figure 9 shows the smoother's performance at estimating these variations with a highly stable oven-controlled crystal oscillator (OCXO) as the receiver clock. Figure 10 shows the smoother's performance at estimating these variations with a temperature compensated crystal oscillator (TCXO) as the receiver clock. During the wardriving effort, an OCXO was used as the receiver clock and thus the original wardriving data were used for the OCXO-based demonstration. However, for the TCXO-based demonstration, the GPS and CDMA observables were modified appropriately to simulate a TCXO as the receiver clock. Specifically, common-mode phase and pseudorange variations commensurate with that caused by a mid-range TCXO were added across all channels.

When compared against the truth model $\hat{\delta t}$ (the GPS-only carrier phase-based estimate of the receiver clock variations), Fig. 9 shows that the smoother had no trouble estimating the OCXO receiver clock variations while ingesting both GPS and CDMA carrier phase measurements. However, when ingesting only CDMA carrier phase measurements, the smoother performance degrades somewhat. In reality, because the receiver clock (an OCXO) varied much less than 1 cycle over the 4-minute segment, its variations were not significantly observable by the smoother, par-

ticularly since the smoother was ingesting measurements from only two CDMA SOPs. The clocks within the CDMA basestations are of OCXO-quality. As a consequence, with only two of these SOPs being ingested during stage 3, the smoother had trouble distinguishing variations of the receiver's clock from variations caused by the CDMA SOP clocks. Nonetheless, as section V-D, will argue, even this seemingly poor estimate of the receiver's variations will be good enough to allow a TCON-based receiver to extend its coherent integration time beyond 100 seconds.

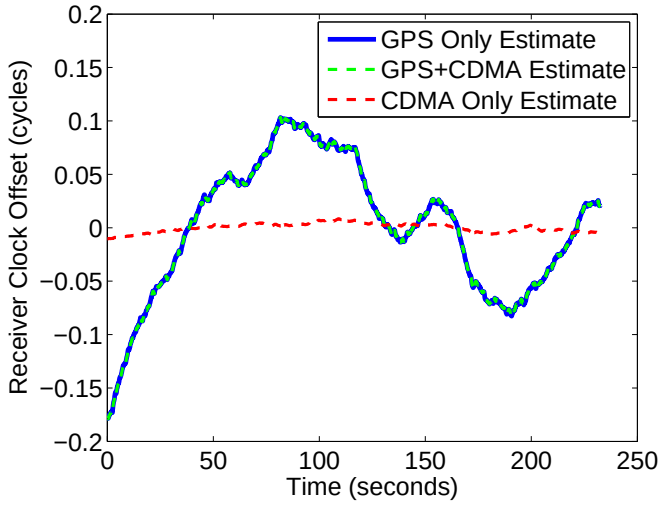

Fig. 9. Receiver clock offset estimates (OCXO).

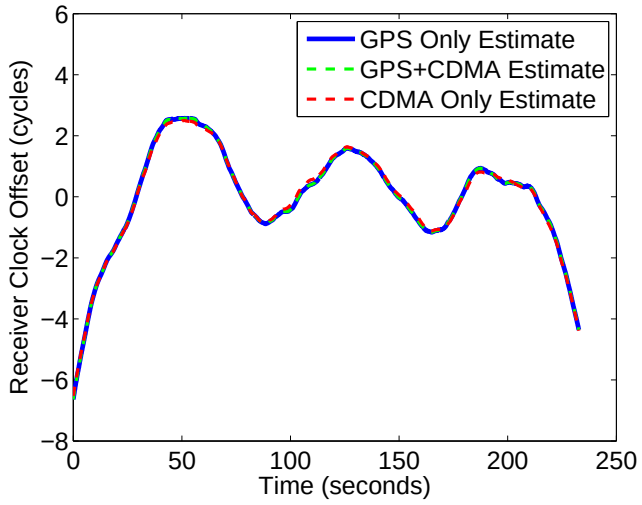

Fig. 10. Receiver clock offset estimates (simulated TCXO).

When compared against the truth model of δt, Fig. 10 shows that the smoother had no trouble estimating the TCXO receiver clock variations while ingesting the carrier phase measurements for both the GPS+CDMA and the CDMA-only situations (stage 2 and 3). Because the receiver clock (a simulated TCXO) varied many cycles over the 4-minute segment, these variations were highly observable by the smoother. This observability arises because, compared with the OCXO-quality clocks within the CDMA basestations, the receiver clock variations were easy to distinguish from those caused by the basestations. Even with only two CDMA signals being ingested, these variations were accurately estimated as evident in Fig. 10. The next section discusses the importance of having a good estimate of receiver clock variations.

D. Results Analysis

In this section, the time history of the CDMA-only receiver clock estimates $\hat{\delta t}_{\mathrm{CDMA}}(t_R)$ will be analyzed for their accuracy. The error in these estimates as a function of receiver time $\tilde{\delta t}(t_R)$ can be defined as the difference of CDMA-based estimate $\hat{\delta t}_{\mathrm{CDMA}}(t_R)$ from the GPS-based "truth" estimate $\hat{\delta t}(t_R)$:

$$\tilde{\delta t}(t_R) = \hat{\delta t}(t_R) - \hat{\delta t}_{\mathrm{CDMA}}(t_R) \tag{13}$$

Coherence time is one simple metric for evaluating the accuracy of clock estimates. Roughly speaking, the coherence time is the amount of time it takes for the phase error

$$\phi_r(t_R) = f_c \cdot \tilde{\delta t}(t_R) \tag{14}$$

(with linear trends removed) to drift more than one-half of a cycle. Eq. (14) is a simple conversion from the receiver clock estimate error $\tilde{\delta t}(t_R)$ to the phase error $\phi_r(t_R)$ where f_c represents the clock's nominal center frequency. Here, f_c = 1575.42 MHz, the GPS L1 C/A carrier frequency. More formally, the coherence time is defined as the time at which the mean-squared coherence function $\langle C^2_{\mathrm{coh}}(\tau)\rangle$ drops below 0.5, where [11]

$$C_{\mathrm{coh}}(\tau) = \left| \frac{1}{\tau} \int_0^{\tau} e^{j\phi_r^{(t)}} dt \right|, \qquad 0 \le C_{\mathrm{coh}}(\tau) \le 1. \tag{15}$$

Figure 11 shows the mean-squared coherence of the estimate errors for both the OCXO and TCXO receiver clocks. $\langle C^2_{\mathrm{coh}}(\tau)\rangle$ could only be plotted out to 200 seconds here because it is limited by the length of data with which it is calculated. Nonetheless, it is apparent, from the figure, that both the OCXO and the TCXO estimate errors have coherence times beyond 100 seconds, since neither trace has by then dipped below 0.5.

As mentioned earlier, the coherence time is a good metric of how well the smoother was able to estimate the receiver clock variations. In fact, the coherence time of the estimate errors is a good measure of how long a receiver can coherently integrate. A receiver provided with an estimate of its local clock variations can use this aiding information

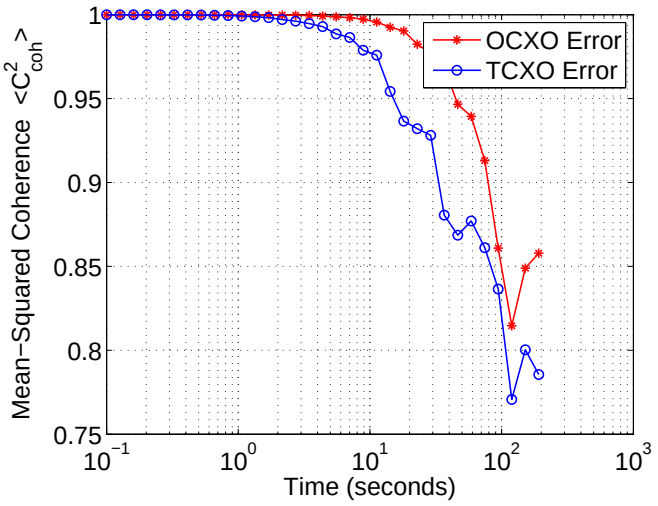

Fig. 11. Mean-squared coherence function calculated for both OCXO and TCXO receiver clock estimate errors.

to remove these variations, allowing it to extend its coherent integration time beyond what its unaided local clock variations would otherwise allow [11]. Because the CDMA-based estimate errors have a coherence time beyond 100 seconds, this implies that post-characterized CDMA signals can be used to supply a TCON-receiver with a coherent integration time beyond 100 seconds.

To acquire a GNSS signal under reasonable acquisition statistics, a receiver must integrate the signal such that the signal-to-noise ratio (SNR) of the coherent accumulations, known as the pre-detection SNR, or $\mathrm{SNR_{PD}}$, surpasses an acquisition threshold of approximately 11 dB. The coherent integration time τ is related to $\mathrm{SNR_{PD}}$, the carrier-to-noise ratio C/N_0 of the received GNSS signal, and $\langle C^2_{\mathrm{coh}}(\tau)\rangle$ by the following equation:

$$\mathrm{SNR_{PD}}(\tau) = \langle C^2_{\mathrm{coh}}(\tau)\rangle \cdot \tau \cdot C/N_0. \qquad (16)$$

Assuming an achievable coherent integration time of 100 seconds ($\tau = 100$), Fig. 11 can be used to approximate a mean-squared coherence lower bound $C^2_{\mathrm{coh}}(100) \approx 0.8$ for both clocks. With these values and an assumed target $\mathrm{SNR_{PD}} = 11$ dB, Eq. (16) can be used to back-calculate a required C/N_0 of at least –8 dB-Hz for reliable GNSS signal acquisition. This means that assuming all else ideal, CDMA-only TCON (post-characterization) will allow GNSS acquisition of signals down to –8 dB-Hz. In a real-world situation, of course, there are many limitations that prevent a receiver from acquiring GNSS signals this weak. Nonetheless, this demonstration has shown that TCON can eliminate a receiver's local clock variations as one of these limitations.

VI. CONCLUSION

A strategy referred to as tightly-coupled opportunistic navigation (TCON) has been presented for exploiting the frequency stability, transmit location, and timing information of ambient radio-frequency "signals of opportunity." The strategy involves a collaborative framework for characterizing these signals and an optimal technique for fusing their observables together. A simple demonstration of TCON on timing has shown that CDMA cellular signals that have been properly characterized by a TCON-enabled receiver can be exploited by the receiver to estimate and remove the effects of its local clock variations, allowing it to extend its coherent integration time beyond 100 seconds.

ACKNOWLEDGMENTS

This work was generously supported in part by the Department of Defense through the National Defense Science and Engineering Graduate (NDSEG) Fellowship Program. Thanks also to Kyle Wesson and Andrew Higdon of The University of Texas at Austin Radionavigation Laboratory for their support in collecting the wardriving data.

References

[1] S. Haykin, "Cognitive radio: brain-empowered wireless communications," *IEEE Journal on selected areas in communications*, vol. 23, no. 2, pp. 201–220, 2005.

[2] R. Rowe, P. Duffett-Smith, M. Jarvis, and N. Graube, "Enhanced GPS: The tight integration of received cellular timing signals and GNSS receivers for ubiquitous positioning," in *Position, Location and Navigation Symposium*. IEEE/ION, 2008, pp. 838–845.

[3] H. Lu, S. Zhang, Y. Dong, and X. Lin, "A Wi-Fi/GPS integrated system for urban vehicle positioning," in *Proceedings of the ION GNSS Meeting*, 2010, pp. 1663 –1668.

[4] J. Do, M. Rabinowitz, and P. Enge, "Performance of hybrid positioning system combining GPS and television signals," in *Position, Location, And Navigation Symposium, IEEE/ION*, 2006, pp. 556–564.

[5] M. Joerger, J. Neale, and B. Pervan, "Iridium/GPS carrier phase positioning and fault detection over wide areas," in *Proceedings of the 22nd International Technical Meeting of The Satellite Division of the Institute of Navigation (ION GNSS 2009)*, pp. 1371–1385.

[6] M. Lashley and D. Bevly, "What are vector tracking loops, and what are their benefits and drawbacks?" *GNSS Solutions Column, Inside GNSS*, vol. 4, no. 3, pp. 16–21, 2009.

[7] E. Ohlmeyer, "Analysis of an ultra-tightly coupled gps/ins system in jamming," in *Position, Location, And Navigation Symposium, IEEE/ION*, 2006, pp. 44 – 53.

[8] M. Psiaki and S. Mohiuddin, "Modeling, analysis, and simulation of GPS carrier phase for spacecraft relative navigation," *Journal of Guidance Control and Dynamics*, vol. 30, no. 6, p. 1628, 2007.

[9] X. Li and Y. Bar-Shalom, "A recursive multiple model approach to noise identification," *Aerospace and Electronic Systems, IEEE Transactions on*, vol. 30, no. 3, pp. 671 –684, jul 1994.

[10] M. Psiaki, "Backward-smoothing extended kalman filter," *Journal of guidance, control, and dynamics*, vol. 28, no. 5, pp. 885–894, 2005.

[11] K. Wesson, K. Pesyna, J. Bhatti, and T. E. Humphreys, "Opportunistic frequency stability transfer for extending the coherence time of GNSS receiver clocks," in *Proceedings of the ION*

GNSS Meeting. Portland, Oregon: Institute of Navigation, 2010.

[12] T. E. Humphreys, J. Bhatti, T. Pany, B. Ledvina, and B. O'Hanlon, "Exploiting multicore technology in software-defined GNSS receivers," in *Proceedings of the ION GNSS Meeting*. Savannah, GA: Institute of Navigation, 2009.

[13] T. E. Humphreys, B. M. Ledvina, M. L. Psiaki, and P. M. Kintner, Jr., "GNSS receiver implementation on a DSP: Status, challenges, and prospects," in *Proceedings of the ION GNSS Meeting*. Fort Worth, TX: Institute of Navigation, 2006.